*Bull. Chem. Soc. Jpn.*, ***74***, *1021—1029 (2001)*

# Electric Field Effects on the Adsorption, Charge Transfer and Vibrational State at Metal Electrodes: A DFT Study on $H_2O$/Pt(111), $H_2O$/Pt(100) and $(H_2O)_2$/Pt(111)

**Tsukuru Ohwaki, Kazuhisa Kamegai, and Koichi Yamashita***

Department of Chemical System Engineering, The University of Tokyo, 7-3-1 Hongo, Bunkyo, Tokyo 113-8656

(Received November 20, 2000)

Electric field (EF) effects on an adsorbed $H_2O$ and $(H_2O)_2$ on Pt(111) and (100) surfaces have been studied using density functional theory (DFT) at the B3LYP/LanL2DZ level. For the interactions between the $H_2O$ and the Pt surface (modeled as a cluster), natural bond orbital (NBO) analysis was performed. This showed that the $H_2O$ interacts strongly with the Pt surface through the higher energy level lone pair of the $H_2O$ in a parallel orientation. Geometry optimizations of the adsorbed water molecule on the Pt(111) surface were carried out, and the changes in the orientation and geometry induced by the EF are discussed. In the cases of EF = 0 and EF > 0, the charge transfer interaction between the $H_2O$ and the Pt surface dominates and the $H_2O$ is adsorbed at the top site. For EF < 0, the interaction between the dipole moment of the $H_2O$ and EF dominates over the charge transfer interaction. Based on the optimized geometries, we have analyzed the vibrational structure and the EF effects on the vibration of the adsorbed $H_2O$. For the $(H_2O)_2$ adsorbed on the Pt(111) surface, partial-optimization calculations have been carried out and the hydrogen bonding in the dimer has been analyzed.

Phenomena at the electrode/electrolyte interface have been understood macroscopically (thermodynamically) so far. However, it has recently been possible to investigate microscopically the phenomena in the vicinity of electrode surfaces by using STM and LEED. Modern electrochemistry is at the stage of designing functional electrode surfaces microscopically. Therefore, a detailed understanding of the electric field effects on adsorption and charge transfer in the vicinity of electrode surfaces is of fundamental importance in electrochemistry.

As one of the most fundamental problems, the adsorption of water molecules on a metal electrode surface has been studied by many researchers in order to understand the structure of the electric double layer in the vicinity of the electrode surface. From the viewpoint of the classical model,[1–3] it is expected that water molecules have an oxygen-up or an oxygen-down orientation at solid–liquid interfaces due to the interaction between the electric field and the dipole moment of the water molecules. This model has succeeded in explaining the electrical capacity of the double layer in the vicinity of electrode surfaces. However, for the purpose of understanding the structure of the electric double layer and the phenomena at electrode–electrolyte interfaces in detail, it is necessary to take into account not only the interaction between water molecules and an electric field, but also between water molecules and electrodes.

Theoretical approaches to the problems of water-electrode interfaces have been undertaken by many researchers for several decades. For example, molecular dynamics (MD)[4,5] and Monte Carlo (MC)[6,7] simulations have been frequently used. In these methods, it is possible to take into consideration the interaction between solvent molecules and adsorbate molecules, and an image charge in the electrodes. On the other hand, molecular orbital theory has been adopted as another approach to investigate water-electrode interfaces. In the 1980s, the extended Hückel method was mainly used, and microscopic understanding of the water-metal electrode interface was achieved in a qualitative way.[8–12] Holloway and Bennemann[9] carried out calculations for the interaction between a water molecule and a cluster-modeled Pt(100) electrode surface. They found that the water molecule interacts with the Pt surface through the oxygen lone-pair orbitals. The interaction energy in the case of four-fold hollow adsorption was larger than the case of on-top adsorption, assuming that water molecules interact with the electrode in oxygen-up and oxygen-down orientations. Estiú and co-workers[11,12] investigated the water decomposition reaction on cluster-modeled Pt(111) and (100) electrode surfaces by using the extended Hückel theory. They simulated the changes in electrode potentials by increasing or decreasing the ionization potentials of metal atoms in their model cluster. They noticed that the on-top adsorption of a water molecule (oxygen-down) is strongest in both cases of Pt(111) and (100) surfaces, and that the interaction energy in the case of Pt(100) is larger than in the case of Pt(111).

Recently, Osawa and co-workers[13] have experimentally investigated a potential dependence of reorientation of water molecules at the interface between an Au(111) electrode surface and an electrolyte by means of surface-enhanced infrared adsorption spectroscopy (SEIRAS). This infrared spectroscopy technique enabled them to observe the electrode-electrolyte interface in detail, removing the influence of the bulk solution and giving new insights into the electric double layer. They reported that the relative populations of orientations of water molecules change with bias voltage around the potential of zero charge (pzc) of the electrode. Ito and co-workers[14] investigated the adsorption of $D_2O$ on Pt(111) by infrared reflection adsorption spectroscopy (IRAS). They found that water molecules form a dimer and a tetramer on the Pt(111) surface at low and high coverage, respectively.

In the present paper, we present a computational study on (1) the electric field effects on the orientation and geometry of an adsorbed water monomer (dimer) at Pt(111) and Pt(100) surfaces and (2) a dominant factor of $H_2O$/Pt surface interactions, by using density functional theory (DFT).

## Calculation Method

In this study, we did not take the structure of the solution directly into account, but approximated the overall electrostatic effects that result from both the structure of the solution in the vicinity of the electrodes and the configuration of the electrode surface by a uniform electric field. Akiyama and Hirata[8] have, however, pointed out that the structure and orientation of adsorbates at interfaces may reflect the microscopic structure of the EF. Therefore, it is necessary to note that our model calculation is the "first step" of the investigation for the EF effects on the orientation and geometry of an adsorbed water monomer and dimer.

Pt(111) and Pt(100) single crystal electrodes have been modeled by a $Pt_{10}$ and a $Pt_{13}$ cluster, respectively (Fig. 1). We used clusters containing two layers in this study. If the second layer is not taken into consideration, we obtained the wrong results, especially in optimization calculations. We emphasize the importance of the second layer in the model clusters (see the next section). The $Pt_{10}$ cluster contains seven atoms in the first layer and three atoms in the second, and the $Pt_{13}$ cluster contains nine atoms in the first layer and four atoms in the second. The nearest Pt–Pt distance is fixed at 2.78 Å. We have used the B3LYP/LanL2DZ method, which uses a Becke-style three-parameter exchange functional,[16] the Lee–Yang–Parr correlation functional and effective core potentials.[16,17] Polarization functions are added to the double zeta basis sets of hydrogen and oxygen atoms. We used a Hamiltonian, as shown in Eq. 1, to obtain Kohn–Sham self-consistent field (SCF) solutions of the electronic wave functions. The Hamiltonian, in the presence of the electric field, $\vec{F}$, is given by

$$H(\vec{F}) = H(\vec{0}) + e\vec{F}\cdot\sum_i \vec{r}_i - e\vec{F}\cdot\sum_j Q_j\vec{R}_j \qquad (1)$$

where $H(\vec{0})$ is the field-free Hamiltonian, $Q_i$ is the charge on the atomic nuclei, and $r_i$ and $R_i$ are electron and nuclear coordinates, respectively. The second term denotes interactions between the electric field and electrons, and the third term represents interactions between the field and atomic nuclei, that is, EF effects are taken into account based on a one-electron operator approximation. This scheme may be called the "finite-field DFT method". This electric-field Hamiltonian has been widely used for HF-SCF calculations.[18–27] A finite electric field of 0.01 au, which corresponds to $5.14 \times 10^7$ V/cm, is in a direction normal to the surface. The sign of the field is chosen so that a positive sign induces a negative charge on the adsorbates (Fig. 1). In the case of EF < 0 and EF > 0, the model clusters correspond to cathode and anode, respectively.

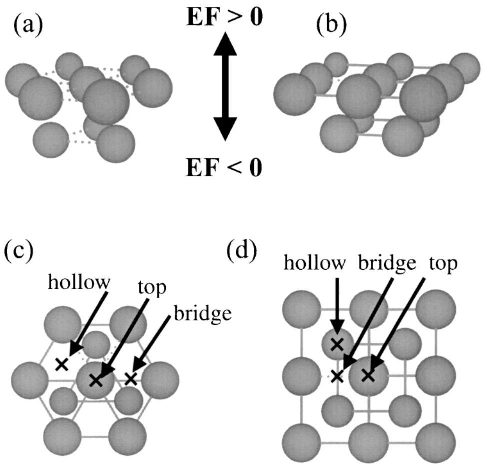

Fig. 1. Models of the Pt electrode surface: (a) model cluster for the Pt(111) electrode surface; (b) model cluster for the Pt(100) electrode surface; (c) adsorption site for the Pt(111) electrode surface; and (d) adsorption site for the Pt(100) electrode surface.

We have carried out single point energy calculations and natural bond orbital (NBO) analysis[28–30] in order to reveal what kinds of interactions are important in $H_2O$/Pt(111) and $H_2O$/Pt(100). By performing an NBO analysis, one can investigate interactions between an adsorbate and a substrate from the viewpoint of orbital-orbital interactions. We have also performed geometry optimization calculations of an adsorbed water monomer at the Pt(111) surface and have investigated geometrical changes induced by an electric field. For vibrational analysis of the adsorbed water molecule, we adopted the GF matrix method. All the DFT calculations and NBO analyses were carried out using the Gaussian94 and Gaussian98 program packages.[31]

## Results and Discussion

**Single Point Energy Calculations of the $H_2O$/Pt(111) and $H_2O$/Pt(100) Surfaces.** We have assumed three orientations of a water molecule adsorbed on the Pt surface: oxygen-down (O-down), parallel, and oxygen-up (O-up) structures (Fig. 2). Three sites, as shown in Fig. 1, have been adopted: top, bridge and three-fold hollow (four-fold hollow in the case of the

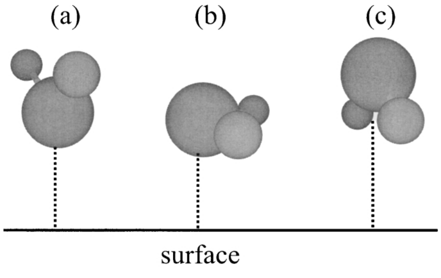

Fig. 2. Orientations of an adsorbed water molecule: (a) oxygen-down; (b) parallel; and (c) oxygen-up.

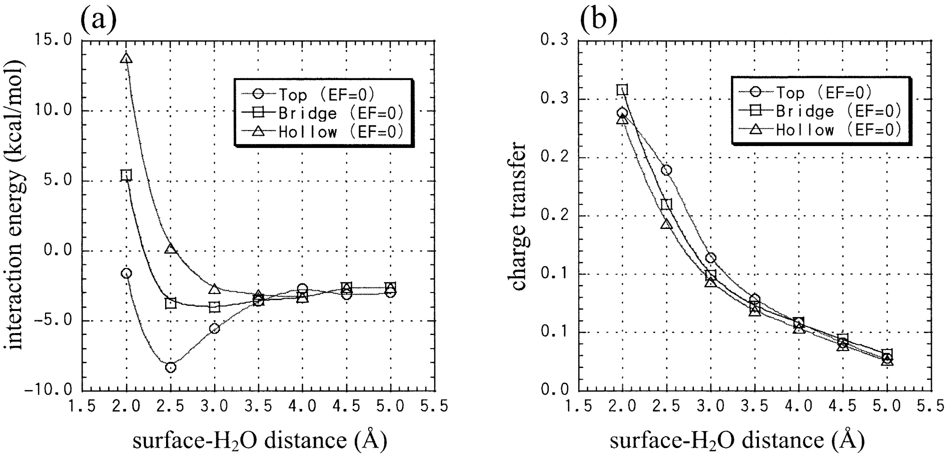

Fig. 3. Interaction energy and charge transfer curves for the $H_2O$(oxygen-down)/Pt(111) interaction system (EF = 0).

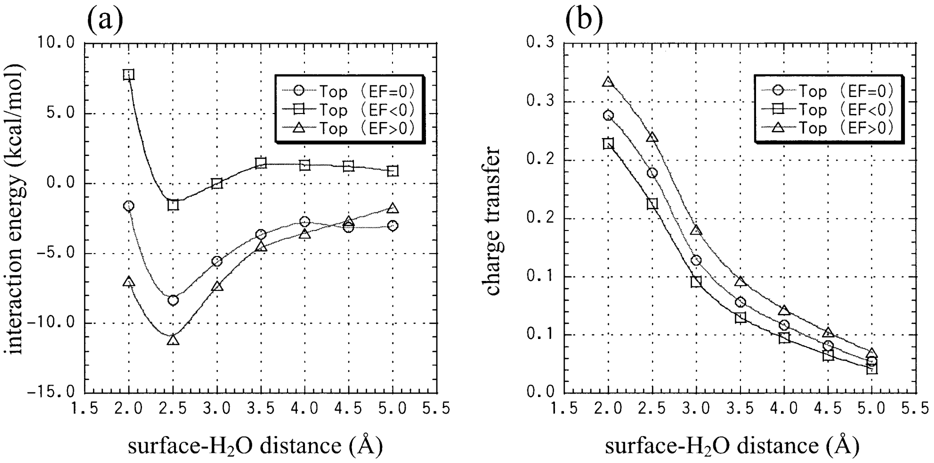

Fig. 4. Interaction energy and charge transfer curves for the $H_2O$(oxygen-down)/Pt(111) interaction under EF = 0, EF > 0 and EF < 0.

Pt(100) surface). In these single point energy calculations, the geometry of the water molecule is fixed; the O–H distance is 0.95 Å, the H–O–H angle is 105.6°, and the O–Pt distance is varied from 2.0 to 3.5 Å in steps of 0.25 Å.

**$H_2O$/Pt(111) Surface.** We begin with the case of the oxygen-down structure. Figure 3a shows the $H_2O$(O-down)–Pt(111) interaction energy curves on the top, bridge and hollow sites with EF = 0. The order of interaction energy for adsorption has been calculated as top > bridge. In the case of the hollow site, a repulsive interaction potential was obtained. This trend does not change whether the EF is zero or not. However, the magnitude of the interaction energy is greatly influenced by the presence of the EF. Figure 4a shows the variation of interaction energy induced by the EF on the top site. The order of the interaction energies is "EF > 0" > "EF = 0" > "EF < 0", and this order is similar to the cases of bridge and hollow.

Figure 3b shows the charge transfer curves on each site when EF = 0. The direction of electron transfer is generally from the adsorbate to the metal surface, and therefore the numbers in the following Figs. (3b, 4b, 5b, 6b, 7b and 8b) correspond to the numbers of electrons that move from the water molecule to the Pt cluster. The calculated results indicate that the bonding between the Pt surface and a water molecule is largely ionic. The order of charge transfer is almost the same as that of the interaction energy in Fig. 3a, and does not depend on the presence of the EF. Figure 4b shows the variation of charge transfer induced by an EF on the top site. The order of charge transfer is "EF > 0" > "EF = 0" > "EF < 0", and this order does not depend on the adsorption site. The point is that electrons move parallel to the direction of the EF, and this order is the same as that of the interaction energy shown in Fig. 4a. We will analyze the interaction in more detail based on the NBO theory in the Section after next.

Let us consider the case of $H_2O$(parallel)/Pt(111) and $H_2O$(O-up)/Pt(111). Figures 5a and 5b show, respectively, the interaction energy and the number of electrons transferring from the water molecule to the Pt cluster for $H_2O$(parallel)/Pt(111). The figures show that both the order of interaction energy and charge transfer with EF = 0 are top > bridge $\simeq$ hol-

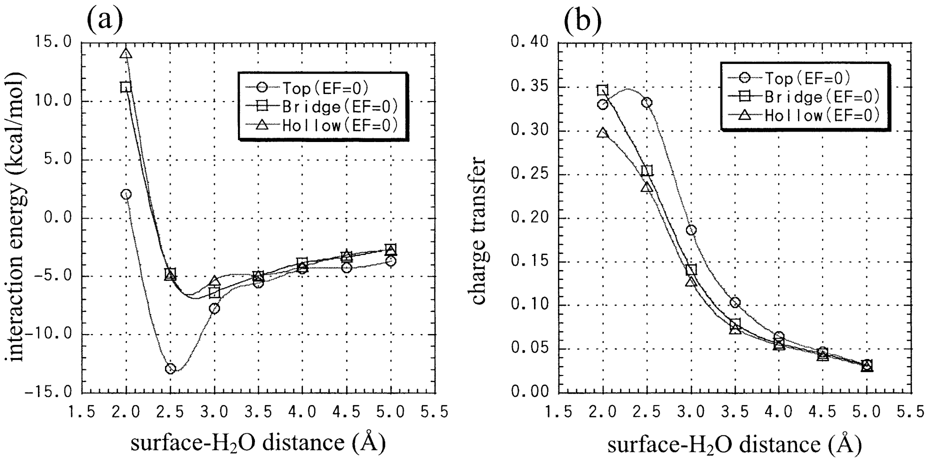

Fig. 5. Interaction energy and charge transfer curves for the $H_2O$(parallel)/Pt(111) interaction system (EF = 0).

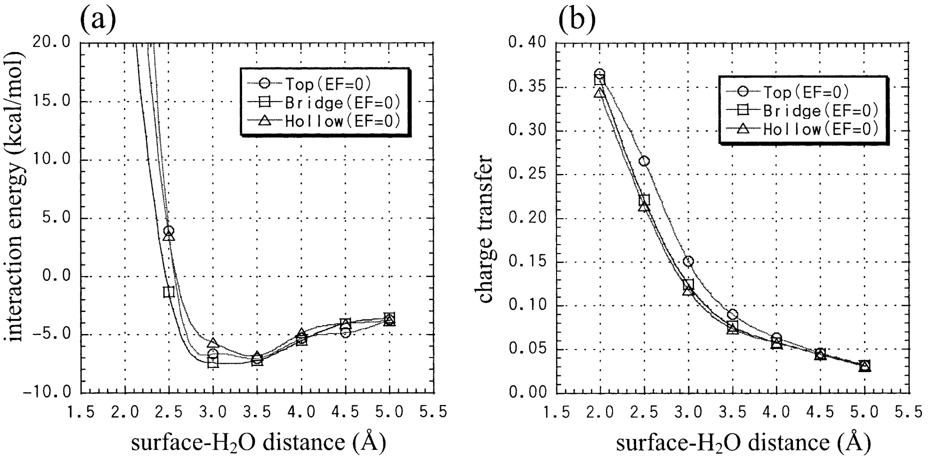

Fig. 6. Interaction energy and charge transfer curves for the $H_2O$(oxygen-up)/Pt(111) interaction system (EF = 0).

low, and therefore it seems reasonable to expect that there is a correlation between the interaction energy and charge transfer. Figures 6a and 6b show, respectively, the interaction energy and the charge transfer for $H_2O$(O-up)/Pt(111). According to Fig. 6a, the interaction energy differs slightly among the sites, and the minimum points of every curve are located apart from the Pt surface, in comparison with those in $H_2O$(O-down)/Pt(111) and $H_2O$(parallel)/Pt(111). This indicates that the interaction between a water molecule and the Pt(111) surface is more physical adsorption-like than in the case when a water molecule has an oxygen-up orientation. The order of charge transfer in Fig. 6b is top > bridge $\simeq$ hollow, which is not in agreement with the order of the interaction energy.

We will make a comparison among the interaction energies of top-site adsorption with EF = 0 (see Fig. 7) in $H_2O$(O-down)/Pt(111), $H_2O$(parallel)/Pt(111) and $H_2O$(O-up)/Pt(111). In the vicinity of the Pt surface (between about 2.0 and 3.0 Å), a water molecule tends to be adsorbed in the parallel conformation. In the case of the O-up orientation, the minimum of the potential energy curve is located relatively far from the surface, and the interaction is that of physical adsorption. In these calculations, however, the orientation of the water molecule was not fully optimized, so it is reasonable to conclude at this

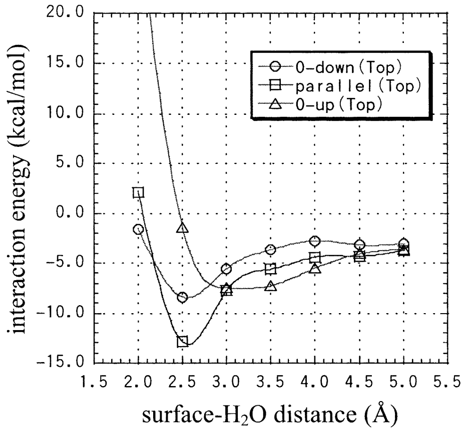

Fig. 7. Interaction energy curves for the $H_2O$(oxygen-down, top-adsorption)/Pt(111), $H_2O$(parallel, top-adsorption)/Pt(111), and $H_2O$(oxygen-up, top-adsorption)/Pt(111) interaction systems (EF = 0).

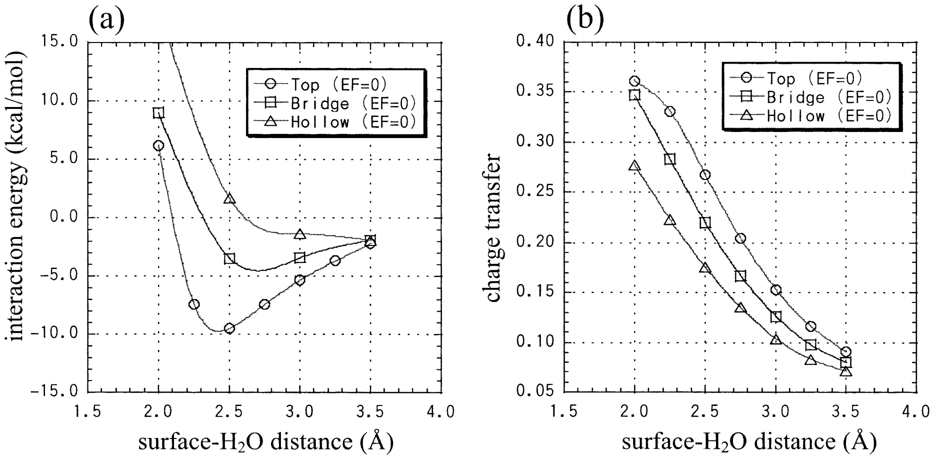

Fig. 8. Interaction energy and charge transfer curves for the $H_2O$(parallel)/Pt(100) interaction system (EF = 0).

stage that the adsorption of a water molecule is in a near-parallel conformation. A full optimization of geometry of an adsorbed water is discussed later.

**$H_2O$/Pt(100) Surface.** As mentioned above, a water molecule interacts strongly with the Pt(111) surface through one of the lone pairs of the water molecule, which is located in the higher energy level, and the water molecule interacts most strongly with the surface in a parallel orientation. In this section, we will discuss the effect of surface structure on the interaction between the Pt surface and a water molecule in a parallel orientation.

Figures 8a and 8b show, respectively, $H_2O$(parallel)/Pt(100) interaction energy curves and the number of electrons transferring from the water molecule to the Pt cluster on each site under EF = 0. The order of interaction energy and the number of transferred electrons have been calculated as top > bridge > hollow sites. A repulsive interaction potential was obtained in the case of hollow-site adsorption. Although these results are similar to the case of $H_2O$(parallel)/Pt(111), the magnitude of the interaction energy for the top-site adsorption at Pt(111) is larger than that for Pt(100) (see Fig. 5a). We will discuss this difference in more detail based on NBO analysis in the next section.

**NBO Analysis for $H_2O$/Pt(111) and $H_2O$/Pt(100).** Estiú and co-workers[11] noticed that the on-top adsorption of a water molecule (O-down) is strongest for both Pt(111) and (100) surfaces, and that the interaction energy in the case of Pt(100) is larger than the case of Pt(111). As for the reason why the on-top adsorption is strongest, they expected that the overlap between the oxygen lone-pair orbital and Pt orbital is larger in the case of the on-top adsorption. However, they did not discuss quantitatively the difference in the interaction energy between adsorption sites and between Pt(111) and (100) surfaces. We discuss this from the viewpoint of orbital-orbital interactions by using NBO analysis.

In NBO analysis,[28–30] a many-electron molecular wavefunction is analyzed in terms of localized electron-pair units, and it is possible to obtain donor-acceptor interaction energies and charge transfers between NBOs. The picture obtained by using NBO analysis corresponds to a chemist's Lewis structure picture.

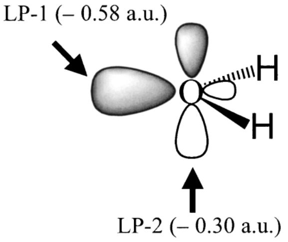

Fig. 9. "One-center" NBOs (lone pairs) of a water molecule. The values in parentheses are the energy levels of the lone pairs.

In Fig. 9, the "one-center" NBOs (lone pairs) of the $H_2O$ molecule are shown. LP-1 and LP-2 are, respectively, a parallel lone pair and a vertical lone pair referred to the H–O–H plane. LP-1 is formed from an $sp^{0.9}$ hybrid (47.3% p-character) on oxygen, while LP-2 is a p atomic orbital (almost 100% p-character). Therefore, the energy level of LP-1 is lower than LP-2 by about 0.3 a.u.. With respect to the NBOs of a Pt cluster, we have obtained a localized NBO on each Pt atom. In the following discussion, however, we will not specify an interaction between the water molecule and each Pt atom, but will treat the Pt cluster as a whole.

In Table 1, the main donor-acceptor interactions between the NBOs of a water molecule and a Pt cluster are summarized. In the case of top-adsorption for $H_2O$(parallel)/Pt(111), this analysis reveals that a significant charge transfer from LP-2 to the Pt cluster occurs. Even in the case of bridge- and hollow-adsorption for $H_2O$(parallel)/Pt(111), it is shown that LP-2 interacts with the Pt cluster. However, the total interaction energy between LP-2 and the Pt cluster for the bridge- and hollow-adsorption do not exceed that of top-adsorption. In the case of $H_2O$(parallel)/Pt(100), the same trend is seen with respect to the difference in interaction energy by adsorption site. In Section 3-1-2, it is shown that the interaction between a water molecule and a Pt(111) cluster for top-adsorption is stronger than that for a Pt(100) cluster. According to Table 1, the magnitude of the interaction between LP-2 and the Pt(111) cluster is larger than that of the Pt(100) cluster. On the whole, the magnitude of charge transfer from a water molecule to a Pt

Table 1. Occupancies of NBO's of Water Molecule and the Main Interactions between Water Molecule and Pt Cluster (EF = 0)

| $H_2O$/Pt(111) | | | | | | |
|---|---|---|---|---|---|---|
| State of adsorption[a)] | | O-down/top/2.5 Å | O-up/top/3.5 Å | Parallel/top/2.5 Å | Parallel/bridge/2.5 Å | Parallel/hollow/2.5 Å |
| Occupancy of NBO's | $\sigma_{O\text{–}H}$ | 1.998 | 1.996 | 1.997 | 1.996 | 1.997 |
| | LP-1 | 1.927 | 1.990 | 1.996 | 1.988 | 1.988 |
| | LP-2 | 1.989 | 1.989 | 1.889 | 1.939 | 1.944 |
| | $\sigma^*_{O\text{–}H}$ | 0.003 | 0.003 | 0.006 | 0.005 | 0.005 |
| Main interactions[b)] | | LP-1 → Pt (9.3) | $\sigma_{O\text{–}H} \rightarrow$ Pt (0.4 × 2) | LP-2 → Pt (24.7)<br>Pt → $\sigma^*_{O\text{–}H}$ (0.6 × 2) | $\sigma_{O\text{–}H} \rightarrow$ Pt (1.6 × 2)<br>LP-1 → Pt (1.5)<br>LP-2 → Pt (11.7)<br>Pt → $\sigma^*_{O\text{–}H}$ (0.7 × 2) | $\sigma_{O\text{–}H} \rightarrow$ Pt (1.1 × 2)<br>LP-1 → Pt (0.9)<br>LP-2 → Pt (9.7) |

| $H_2O$/Pt(100) | | | | | | |
|---|---|---|---|---|---|---|
| State of adsorption[a)] | | Parallel/top/2.5 Å | Parallel/bridge/2.5 Å | Parallel/hollow/2.5 Å | | (Isolated $H_2O$) |
| Occupancy of NBO's | $\sigma_{O\text{–}H}$ | 1.997 | 1.996 | 1.997 | | 2.000 |
| | LP-1 | 1.996 | 1.988 | 1.990 | | 1.999 |
| | LP-2 | 1.893 | 1.939 | 1.961 | | 1.998 |
| | $\sigma^*_{O\text{–}H}$ | 0.004 | 0.004 | 0.005 | | 0.000 |
| Main interactions[b)] | | $\sigma_{O\text{–}H} \rightarrow$ Pt (3.2 × 2)<br>LP-1 → Pt (2.0)<br>LP-2 → Pt (17.0) | $\sigma_{O\text{–}H} \rightarrow$ Pt (0.7 × 2)<br>LP-1 → Pt (2.5)<br>LP-2 → Pt (7.6) | $\sigma_{O\text{–}H} \rightarrow$ Pt (1.2 × 2)<br>LP-1 → Pt (3.4)<br>LP-2 → Pt (0.6) | | |

a) Orientation of water molecule/adsorption site/adsorption length.

b) Values in parentheses represent corresponding interaction energies in kcal mol$^{-1}$.

cluster is almost proportional to the interaction energy. These results suggest that the interaction between a water molecule and a metal surface occurs through the lone pair of the water molecule, and that the lone pair of the water molecule interacts most strongly with the Pt atom in the case of top-adsorption. We may conclude that charge transfer is one of the most important factors that determine adsorption structures and adsorption sites when the interaction between a lone pair of a water molecule and a Pt surface dominates in the interaction energy.

Why is the interaction energy on the top site for $H_2O$(parallel)/Pt(111) larger than those of the top site for $H_2O$(O-down)/Pt(111) and $H_2O$(O-up)/Pt(111)? An $H_2O$(O-up) molecule interacts with a Pt cluster though $\sigma_{O\text{-}H}$ orbitals. However, this interaction energy is very small. LP-1 and LP-2 mainly interact with the Pt cluster through O-down and parallel orientations, respectively. The energy level of LP-2 (− 0.3 a.u.) is closer to that of the half-occupied 6s(Pt) orbital (− 0.29 a.u.) than to that of LP-1 (− 0.58 a.u.), and LP-2 can interact more strongly with the 6s(Pt) orbital. In $H_2O$(parallel)/Pt(111), the water molecule interacts with the cluster through LP-2, and therefore the interaction energy is larger than that of $H_2O$(O-down)/Pt(111). Comparing the 6s(Pt) orbitals between $H_2O$(parallel)/Pt(111) and $H_2O$(parallel)/Pt(100), we can explain the result that the interaction energy on the top site for $H_2O$(parallel)/Pt(111) is larger than that of $H_2O$(parallel)/Pt(100), since the energy level of the 6s(Pt) orbital of the Pt(100) surface (− 0.17 a.u.) is higher than that of Pt(111).

**Geometry Optimization for an Adsorbed $H_2O$ Molecule on Pt(111).** In this section, we describe a full geometry optimization for an $H_2O$ molecule on the Pt(111) surface in order to discuss in detail the structure of the adsorbed $H_2O$ molecule on a Pt(111) surface and electric field effects. Based on the result in Section 3-1, (1) the adsorption site of the $H_2O$ molecule is fixed at the top site, (2) geometry optimizations are started from a configuration such that the H–O–H plane is parallel to the Pt surface and (3) all of the internal structure of the $H_2O$ molecule and the adsorption length between the water molecule and the Pt surface are relaxed.

Here, we should note that the orientations of the adsorbed $H_2O$ molecules obtained by geometry optimizations were O-up and parallel respectively for a one-layer $Pt_7$ and a two-layer $Pt_{10}$ cluster (under EF = 0). This is due to the difference in the localization of charge in each cluster. That is, in the case of the one-layer cluster, all electrons transferring from $H_2O$ are localized at the surface of the cluster because of no second-layer, and therefore an electrostatic interaction between the positive charge of hydrogens of $H_2O$ and the negative charge of the cluster is overestimated resulting in O-up orientation. In this way, especially in the case that a relatively large charge transfer occurs, it is indispensable to use two-layer clusters.

The optimized structures for (a) EF = 0, (b) EF > 0 and (c) EF < 0 are shown in Fig. 10. In the case of EF = 0, the angle between the H–O–H plane and the normal to the surface has been calculated to be 106.3°. This indicates that the interaction is dominated by LP-2 of the $H_2O$ molecule. Holloway and coworkers[9] reported that their model calculations of water adsorption on a Pt(100) surface yielded little change in the equilibrium H–O–H angle of the adsorbed water molecule as compared with the structure in the gas phase, whereas we, on the contrary, obtained a 1.2° increase. According to our results, the electron transfer from $H_2O$ to the Pt surface in the Pt–$H_2O$ interaction system is relatively large; therefore, it is reasonable to have significant geometrical changes in the adsorbed water molecule.

When EF > 0, the angle shifts to 131.0°, and the adsorption length is shorter than that for EF = 0. In this case, although the interaction of LP-2 with the Pt surface is still dominant, the interaction between the dipole moment of the water molecule and the EF modifies the orientation of the water molecule.

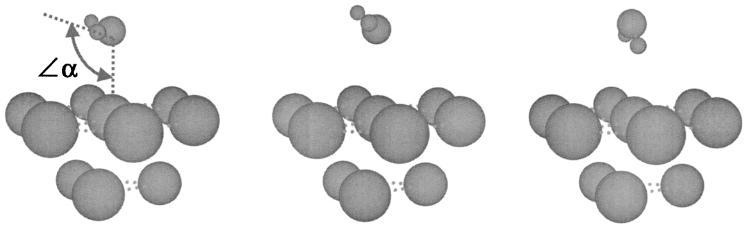

| EF = 0 | EF > 0 | EF < 0 |
|---|---|---|
| O-Pt length : 2.38 Å | O-Pt length : 2.27 Å | O-Pt length : 3.32 Å |
| O-H length : 0.97 Å | O-H length : 0.97 Å | O-H length : 0.97 Å |
| H-O-H angle : 106.5° | H-O-H angle : 107.5° | H-O-H angle : 101.8° |
| H-O-Pt angle : 99.7° | H-O-Pt angle : 112.8° | H-O-Pt angle : 50.9° |
| ∠α : 106.3° | ∠α : 131.0° | ∠α : 1.1° |

Fig. 10. Difference in geometry and orientation of adsorbed water molecule by the direction of the EF, obtained by partial-geometry optimizations. $\angle\alpha$ represents an angle between a molecular plane of a water molecule and a normal to a surface.

Table 2. Force Constants and Frequencies of Water Molecule Adsorbed on Pt(111) Surface

| | Force constants (N/m) | | Symmetric stretch of O–H ($\mathrm{cm}^{-1}$) | Bending of H–O–H ($\mathrm{cm}^{-1}$) | Antisymmetric stretch of O–H ($\mathrm{cm}^{-1}$) |
|---|---|---|---|---|---|
| | O–H | H–O–H | | | |
| isolated | 852.8 | 69.6 | 3877.9 | 1645.8 | 3937.2 |
| EF = 0 | 771.0 | 70.6 | 3685.0 | 1646.6 | 3746.3 |
| EF < 0 | 779.4 | 84.2 | 3713.9 | 1792.1 | 3757.7 |
| EF > 0 | 703.4 | 69.6 | 3518.1 | 1636.1 | 3579.9 |

Moreover, the short O–Pt distance indicates that the interaction between the water molecule and the Pt surface is stronger than in the case of EF = 0. When EF < 0, on the other hand, the water molecule has an O-up orientation. The geometrical configuration is therefore determined by the dipole-EF interaction instead of the interaction between LP-2 and the Pt surface. When the orientation of the water molecule changes from parallel to O-down, LP-1 and LP-2 always locate between the oxygen atom and the Pt cluster. When the water molecule has an O-up orientation, however, neither LP-1 nor LP-2 participate in the interaction. Therefore, in the case of EF > 0, the water molecule interacts with the Pt cluster through LP-2 or a hybridized orbital of LP-1 and LP-2, keeping a parallel-orientation.

With regard to the internal structure of the water molecule, although there is little change in the O–H length, the H–O–H angle depends on the direction of the EF. When EF > 0, the H–O–H angle is 107.5°, which is larger by 1.0° than in the case of EF = 0. When EF < 0, the H–O–H angle is smaller by about 5.0° than in the case of EF = 0. In the case of EF < 0, the water molecule changes its structure to increase the dipole moment and to interact more strongly with the EF. In the case of EF > 0, however, the direction of geometrical change is opposite to the case of EF < 0. The difference in these geometrical changes may be due to the weakness of the interaction between the water molecule and the Pt cluster (physical adsorption) in the case of EF < 0. The structure is relatively easy to change in order to interact more strongly with the EF.

**Vibrational Analysis for $H_2O$/Pt(111).** In this section, we discuss the electric field effects on the vibrational structure of a water molecule adsorbed at a Pt(111) surface. We have calculated the normal vibrational frequencies of an adsorbed water molecule based on the GF matrix method using the numerical second derivatives with respect to the H–O bond length and the H–O–H bond angle. These second derivatives were obtained within a harmonic approximation. The potential energies were fitted to a second-order polynomial on four points (width of scanning; $\Delta r_{\mathrm{O-H}} = 0.005$ Å, $\Delta\theta_{\mathrm{H-O-H}} = 1.0°$) around the potential minimum shown above.

In Table 2, the normal vibrational frequencies of the adsorbed and isolated water molecule are summarized. As compared with the isolated water molecule, the frequencies of the symmetric and antisymmetric stretch of the adsorbed water molecule (EF = 0) are smaller by about 180 $\mathrm{cm}^{-1}$. This change is attributable to a weakening of the O–H bonds due to the electron transfer from the $\sigma_{\mathrm{O-H}}$ orbitals to the Pt cluster and from the Pt cluster to $\sigma^*_{\mathrm{O-H}}$ orbitals (see Table 1). The order of frequency change in the symmetric stretch agrees with that of the electron transfer from the water molecule to the Pt cluster. Therefore, a decrease of electrons in the water molecule leads to a weakening of the O–H bonds, as seen in the frequency analysis for the $H_2O^+$ molecule. In comparison with the case of EF = 0, the frequencies of the symmetric stretch and bending mode for EF < 0 increase by about 30 $\mathrm{cm}^{-1}$ and 150 $\mathrm{cm}^{-1}$, respectively. On the other hand, those frequencies for EF > 0 are smaller than those for EF = 0 by 170 $\mathrm{cm}^{-1}$ and 10 $\mathrm{cm}^{-1}$. The force constant for the bending mode of an adsorbed water molecule increases as compared with that of an isolated water molecule. This result can be attributed to the charge at the hydrogen atoms of the water molecule. According to the Mulliken charge analysis, the charges at the hydrogen atoms of the isolated and adsorbed water molecules are 0.32 and 0.38, respectively. Therefore, the repulsive interaction between the two hydrogen atoms in the adsorbed water molecule is consid-

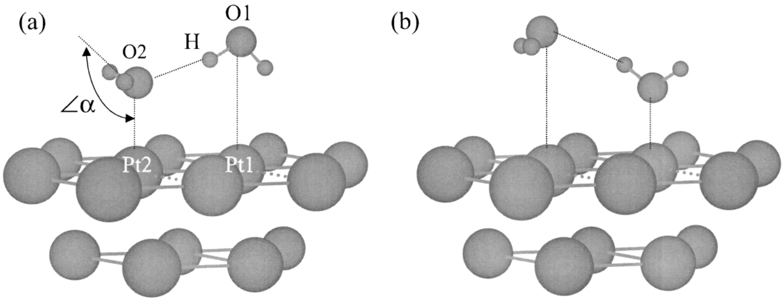

Fig. 11. Initial geometries for the partial-optimization calculations of the water dimer molecule adsorbed on the Pt(111) surface model cluster.

Table 3. Geometries of $H_2O$–$H_2O$ Dimers Adsorbed on Pt(111) Surface and in Gas Phase

| | Distances (Å) | | | Angles (degree) | | |
|---|---|---|---|---|---|---|
| | O1–Pt1 | O2–Pt2 | O2–H | ∠α | ∠H–O1–Pt1 | ∠O1–H–O2 |
| structure (a)[a)] | 3.35 | 2.37 | 1.99 | 108.1 | 63.0 | 146.1 |
| gas phase | — | — | 1.89 | — | — | 173.9 |

a) See Fig. 11.

ered to be stronger than that in the isolated water molecule. The H–O–H angle changes due to the directions of the EF, and the interaction between a water molecule and the Pt surface. The repulsive interaction between two hydrogen atoms of an adsorbed water molecule is also expected to change due to the change of the H–O–H angle. Figure 10 and Table 2 show the correlation between the H–O–H angle and the corresponding force constant. That is to say, the repulsive interaction, and therefore the force constant for the bending mode, increase with the decrease in H–O–H angle. Holloway and co-workers[9] investigated the bending vibration of a water molecule adsorbed on a model-cluster Pt(100) surface. They calculated the force constant of the bending vibration by changing the H–O–H angle (under EF = 0). They obtained a 6% increase in the force constant for the bending vibration of the adsorbed water molecule relative to that in the gas phase, which we also confirm.

**$H_2O$–$H_2O$ Dimer/Pt(111).** Recently, an $H_2O$–$H_2O$ dimer adsorbed on a metal surface has been experimentally studied by Ito and co-workers.[14] By use of IRAS, they found that the structure of water molecules on the Pt(111) surfaces is a dimer and a tetramer at low and high coverage, respectively. They showed that the acceptor water molecule in an $H_2O$–$H_2O$ dimer is adsorbed on the Pt(111) surface in such a way that the oxygen atom is almost parallel to the surface. In this section, we discuss a water dimer on the Pt(111) cluster, that is, (1) the difference in the $H_2O$–$H_2O$ interaction between the case of the gas phase and on a Pt(111) surface and (2) the adsorption structure of an $H_2O$–$H_2O$ dimer on the Pt(111) surface. We have used models as shown in Fig. 11, where the Pt(111) surface is modeled by a two-layer cluster consisting of 15 Pt atoms. Partial-optimization calculations have been carried out by relaxing the O1–surface distance, the O2–surface distance, the H–O1–surface angle, the O1–Pt1–Pt2 and O2–Pt2–Pt1 angles and the $H_2O(2)$ plane–surface angle, with the H-O-H angles (105.6°) and the H–O bond lengths (0.9667 Å) fixed. The initial geometries for the partial-optimization calculations are shown in Figs. 11a and b, where the dimer adsorbed on the Pt(111) cluster has (a) the structure of an $H_2O$–$H_2O$ dimer in the gas phase and (b) the upside-down structure.

In the case of starting with initial structure (b), the partial-optimization calculation did not converge and we could not obtain any meaningful structures. On the other hand, starting with initial structure (a), we obtained the structure of the $H_2O$–$H_2O$ dimer adsorbed on the Pt(111) surface, which is similar to structure (a). This supports the experimental result by Ito and co-workers.[14] It is considered that such a structure results mainly from hydrogen-bonding between $H_2O(1)$ and $H_2O(2)$. According to the NBO analysis, this hydrogen bonding consists of the LP-1 of $H_2O(1)$ and $\sigma^*_{\text{H–O}}$ of $H_2O(2)$. The LP-1-$\sigma^*_{\text{H1–O}}$ interaction energies between $H_2O(1)$ and $H_2O(2)$ are calculated to be 13.6 and 7.7 kcal mol$^{-1}$, for the gas phase case and for structure (a), respectively. This result indicates that the interaction in the $H_2O$–$H_2O$ dimer decreases on the Pt surface. This weakening of the hydrogen bond may result from a repulsive electrostatic interaction. That is, $H_2O(2)$ loses some electrons through a strong interaction of LP-2 with the Pt surface (as mentioned above) to take a positive charge. This positive charge of $H_2O(2)$ interacts repulsively with the hydrogen atom of $H_2O(1)$ and therefore the hydrogen bonding between two water molecules is weakened. In fact, the interaction between $H_2O(2)$ and the Pt(111) surface is still strong even in the $H_2O$–$H_2O$ dimer (LP-2 → Pt: 29.3 kcal/mol), and the distance between $H_2O(1)$ and $H_2O(2)$ adsorbed on the Pt(111) surface is longer than in the gas phase case (see Table 3). As a consequence, an $H_2O$–$H_2O$ dimer is adsorbed on the Pt(111) surface in such a way that an acceptor water molecule interacts strongly with the Pt(111) surface to be almost parallel to the surface. The hydrogen bonding between two water molecules on the surface is weaker than in the gas phase case because of a repulsive interaction between two water molecules that results from a strong interaction between the acceptor water molecule and the Pt(111) surface.

## Conclusions

We studied electric field (EF) effects on an adsorbed water monomer and dimer on the Pt(111) and (100) surfaces by using DFT (B3LYP/LanL2DZ level), this being the first DFT study for an adsorbed water molecule on Pt surfaces, as far as we know. The Pt surface was modeled by a cluster. According to the NBO analysis for the interaction between the water molecule and the Pt surface, the water molecule interacts strongly with the Pt surface through LP-2 (the higher energy level lone pair) of the water molecule and takes a parallel orientation. We have also found a correlation between the interaction energy and the charge transfer for $H_2O$/Pt. Geometry optimizations of an adsorbed water molecule on the Pt(111) surface have been carried out, and the change in the orientation and geometry induced by the EF is discussed. In the case of EF = 0 and EF > 0, the charge transfer interaction between the water molecule and the Pt surface dominates and the water molecule is adsorbed at the top site. On the other hand, for EF < 0, the interaction between the dipole moment of the water molecule and the EF is dominant over the charge transfer interaction. Based on the optimized geometries, we have analyzed the vibrational structure of the adsorbed water molecule on the Pt(111) surface and the EF effects on the vibrational structure by using the GF matrix method. It is shown that the vibrational structure of the adsorbed water molecule on the Pt(111) surface can be influenced by the change in the geometry of the water molecule and the electronic structure, which are induced by the EF and the interaction between the water molecule and the Pt surface. For the water dimer adsorbed on the Pt(111) surface, partial-optimization calculations have been carried out and the hydrogen bonding in the dimer was analyzed. These calculations show that the acceptor water molecule in an $H_2O$–$H_2O$ dimer interacts with the surface through the lone pair of the oxygen atom, and the plane of the acceptor water molecule is almost parallel to the Pt(111) surface. The hydrogen bond in the adsorbed $H_2O$–$H_2O$ dimer on the Pt surface is found to be weaker than in the gas phase case, which is attributable to a repulsive interaction between two water molecules resulting from a strong interaction between the acceptor water molecule and the Pt(111) surface.

This work is supported by Grants-in-Aid for Scientific Research on Priority Area of "Electrochemistry of Ordered Interfaces" from the Ministry of Education, Science, Sports and Culture (#09237216, #10131213, #11740316), and by CREST (Core Research for Evolutional Science and Technology) of Japan Science and Technology Corporation (JST).

### References

1 B. B. Damaskin and A. N. Frumkin, *Electrochim. Acta*, **19**, 173 (1974).

2 R. Parsons, *J. Electroanal. Chem.*, **59**, 229 (1975).

3 W. R. Fawcett, S. Levine, R. M. deNobriga and A. C. McDonald, *J. Electroanal. Chem.*, **111**, 163 (1980).

4 E. Spohr, *J. Phys. Chem.*, **93**, 6171 (1989).

5 N. Goto, T. Kakitani, T. Yamato, and Y. Hatano, *J. Phys. Soc. Japan*, **68**, 3729 (1999).

6 X. Xia, L. Perera, E. Essemann, and M. L. Berkowitz, *Surf. Sci.*, **335**, 401 (1995).

7 N. G. Parsonage and D. Nicholson, *J. Chem. Soc.*, **83**, 663 (1987).

8 R. Akiyama and F. Hirata, *J. Chem. Phys.*, **108**, 4904 (1998).

9 S. Holloway and K. H. Bennemann, *Surf. Sci.*, **101**, 327 (1980).

10 A. B. Anderson and N. K. Ray, *J. Phys. Chem.*, **86**, 488 (1982).

11 G. L. Estiú, S. A. Maluendes, E. A. Castro, and A. J. Ariva, *J. Phys. Chem.*, **92**, 2512 (1988).

12 G. L. Estiú, S. A. Maluendes, E. A. Castro, and A. J. Arvia, *J. Electroanal. Chem.*, **284**, 289 (1990).

13 K. Ataka and M. Osawa, *J. Phys. Chem.*, **100**, 10664 (1996).

14 M. Nakamura, Y. Shingaya, and M. Ito, *Chem. Phys. Lett.*, **309**, 123 (1999).

15 A. D. Becke, *J. Chem. Phys.*, **98**, 5648 (1993).

16 C. Lee, W. Yang, and R. G. Parr, *Phys. Rev. B*, **37**, 785 (1988).

17 B. Miehlich, A. Savin, H. Stoll, and H. Preuss, *Chem. Phys, Lett.*, **157**, 200 (1989).

18 X. Xu, D. Y. Wu, B. Ren, H. Xian, and Zhong-Qun Tian, *Chem. Phys. Lett.*, **311**, 193 (1999).

19 M. Head-Gordon and J. C. Tully, *Phys. Rev. B*, **46**, 1853 (1992).

20 A. B. Anderson, *J. Electroanal. Chem.*, **280**, 37 (1990).

21 D. K. Lambert, *J. Chem. Phys.*, **89**, 3847 (1988).

22 G. Pacchioni and P. S. Bagus, *Phys. Rev. B*, **40**, 6003 (1989).

23 P. S. Bagus, C. J. Nelin, K. Hermann, and M. R. Philpott, *Phys. Rev. B*, **36**, 8169 (1989).

24 P. S. Bagus, C. J. Nelin, W. Müller, M. R. Philpott, and H. Seki, *Phys. Rev. Lett.*, **58**, 559 (1989).

25 M. R. Philpott, P. S. Bagus, C. J. Nelin, and H. Seki, *J. Electron Spectrosc. Relat. Phenom.*, **45**, 169 (1987).

26 S. Holloway and J. K. Nørskov, *J. Electroanal. Chem.*, **161**, 193 (1984).

27 C. Korzeniewski, S. Pons, P. P. Schmidt, and M. W. Severson, *J. Chem. Phys.*, **85**, 4153 (1986).

28 J. P. Foster and F. Weinhold, *J. Am. Chem. Soc.*, **102**, 7211 (1980).

29 A. E. Reed, L. A. Curtiss, and F. Weinhold, *Chem. Rev.*, **88**, 899 (1988).

30 F. Weinhold and J. E. Carpenter, in, R. Naaman and Z. Vager (eds), "The Structure of Small Molecules and Ions," Plenum, New York (1988), pp. 227.

31 M. J. Frisch, G. W. Trucks, H. B. Schlegel, P. M. W. Gill, B. G. Johnson, M. A. Robb, J. R. Cheeseman, T. Keith, G. A. Petersson, J. A. Montgomery, K, Raghavachari, M. A. Al-Laham, V. G. Zakrzewski, J. V. Ortiz, J. B. Foresman, J. Cioslowski, B. B. Stefanov, A. Nanayakkara, M. Challacombe, C. Y. Peng, P. Y. Ayala, W. Chen, M. W. Wong, J. L. Andres, E. S. Replogle, R. Gomperts, R. L. Martin, M. Gordon, C. Gonzalez, and J. A. Pople, "Gaussian 94, Rev. **D.1**," Gaussian Inc., Pittsburgh, PA (1995).